Journal of Raman Spectroscopy

WILEY

Journal of RAMAN SPECTROSCOPY

MINI REVIEW

Plasmon Nanofocusing for Tip-Enhanced Raman Spectroscopy: Principles, Strategies, and Applications

Takayuki Umakoshi | Prabhat Verma

Department of Applied Physics, The University of Osaka, Suita, Japan

Correspondence: Prabhat Verma (verma@ap.eng.osaka-u.ac.jp)

Received: 31 August 2025 | **Revised:** 11 October 2025 | **Accepted:** 14 October 2025

ABSTRACT

Plasmon nanofocusing has emerged as a powerful optical technique for achieving extreme confinement of electromagnetic fields at the nanometer scale by adiabatically compressing propagating surface plasmon polaritons along tapered metallic waveguides. Compared to traditional methods of confining propagating light into a nanometric volume using optical nanoantennas, this alternative approach offers several advantages, including a background-free light source directly at the nanoscale and broadband capabilities, enabling diverse applications in nano-optics and nanoscopy. This review covers the physical principles of plasmon nanofocusing, along with experimental strategies for efficient coupling, with a particular emphasis on grating-assisted and single-slit-assisted excitation, which enable broadband nanofocusing. Its integration with near-field scanning optical microscopy and tip-enhanced Raman spectroscopy, techniques that have revolutionized nanoscale vibrational imaging, has been revisited. We examine progress across various implementations, considering spatial resolution, bandwidth, and field enhancement, and highlight emerging opportunities in ultrafast spectroscopy, single-molecule detection, and quantum plasmonics. Challenges such as tip fabrication precision and coupling efficiency are also discussed.

1 | Introduction

The ability to confine light to dimensions far below its diffraction limit has been a longstanding goal in nanooptics and nanophotonics. This was successfully achieved by utilizing plasmonics, wherein the collective oscillations of free charge carriers (plasmons) in metallic nanostructures, which work as optical nanoantennas, are exploited to manipulate and confine light at the nanoscale through localized surface plasmon resonance (LSPR) [1, 2]. This led to the development of several new optical nanoimaging and nano-optical techniques, including near-field scanning optical microscopy (NSOM) [3, 4] and tip-enhanced Raman spectroscopy (TERS) [5–7]. Traditional NSOM and TERS setups utilize a metallic conical nanotip as an optical nanoantenna, with either smooth [8] or granular surfaces [9, 10], to confine light at its apex. Besides confining the light field, it is also crucial to significantly enhance the light intensity at the apex of the plasmonic tips, which has been a major focus in TERS research. In this context, Johnson et al. [11] and Vasconcelos et al. [12] developed highly reproducible truncated pyramidal plasmonic tips, where the field enhancement could be drastically improved by tuning the plasmon resonance of the tip. In a conventional TERS measurement, the plasmonic tip is placed directly over the sample, and then the tip apex is illuminated by a far-field laser to resonantly excite localized plasmons at the tip apex, thereby generating a near-field confined light at the tip apex [13–15]. Although this configuration facilitates near-field nanoimaging and nanospectroscopy, it inherently necessitates direct illumination of the sample beneath the tip apex with a much larger diffraction-limited far-field illumination, producing substantial unwanted background scattering originating from the laser focal spot. Such background often overwhelms the weak near-field signal, thereby diminishing sensitivity and reducing the signal-to-noise ratio, especially when the sample is a weak scatterer. A practical solution to this problem involves employing some type of noise subtraction method, such as taking measurements twice: once with tip-in, which captures both background scattering and near-field signal, and once with tip-out, which captures

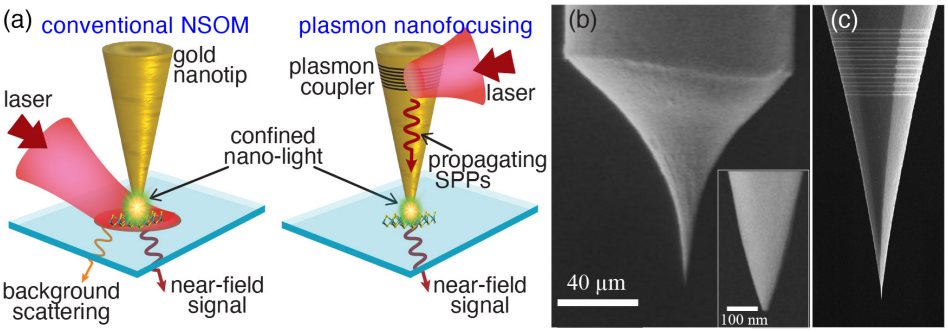

FIGURE 1 | (a) Illumination schemes in a conventional NSOM and a nanofocusing-type NSOM. (b) SEM image of an electrochemically etched solid gold tip with its zoomed-in apex in the inset [16]. (c) SEM image of an electrochemically etched solid gold tip with a grating-type plasmon coupler [17].

only background scattering. These two signals are then subtracted to isolate the near-field signal. However, this approach does not facilitate the retrieval of weak near-field signals that are masked by the background signal. Another key issue is that although LSPRs in metallic nanostructures have long served as the foundation of nanoscale optics, their inherent limitation lies in their resonant nature, which restricts optical enhancement to a narrow bandwidth. As a result, their applicability is restricted to single-wavelength or narrowly tuned optical phenomena.

Plasmon nanofocusing, which has gained increasing attention in recent years, presents an alternative method for confining light and addressing the previously mentioned issues with a fundamentally different approach to concentrate light energy into a nanoscale spatial region at the apex of a tapered metallic structure, such as a metallic wedge or a nanotip used in NSOM and TERS. In this approach, instead of directly illuminating the tip apex, the excitation laser illuminates a plasmon coupler fabricated at a remote location on the taper body, away from the apex. The plasmon coupler compensates for the momentum mismatch between the propagating light and the plasmons, enabling smooth energy transfer from photons to surface plasmons. These excited surface plasmon polaritons (SPPs) then propagate toward the taper apex, adiabatically compressing the electromagnetic energy into a nanometric volume at the apex, ultimately generating a robust localized near-field light at the apex without the need for direct laser illumination of the apex. Figure 1a shows illumination schemes in plasmon nanofocusing-type NSOM compared to the traditional NSOM setup. Reviews by Groß et al. [18] and Lu et al. [19] introduce and consolidate plasmon nanofocusing as a promising new method in nano-optics. The authors in Ref. [18] highlight the analogy between plasmon nanofocusing and a "gray hole" for light, whereby electromagnetic energy is concentrated into an extremely small volume below 10 nm, analogous to a gravitational collapse.

The plasmon coupler in this technique is generally fabricated several micrometers away from the apex, spatially separating it from the apex, ensuring that the sample molecules beneath the tip apex are illuminated solely by the near-field light. This completely eliminates the background scattering typically seen in traditional NSOM and TERS measurements, yielding a cleaner and more sensitive optical signal. Unlike noise-suppression techniques such as modulation methods [20, 21] or subtraction schemes [22], which reduce but do not completely eliminate unwanted scattering, plasmon nanofocusing ideally produces a background-free near-field optical signal. This unique property has been a key factor in the growing interest in plasmon-nanofocusing-based NSOM, TERS, or other applications. Furthermore, unlike optical antennas, where light confinement depends on plasmon resonance [23, 24], plasmon nanofocusing relies on the propagation of SPPs along the tapered metallic structure, while adiabatically compressing the electromagnetic energy as they propagate toward the apex [25]. Since this process depends on propagation rather than the resonance of localized plasmons, it is fundamentally independent of the incident wavelength and can, in principle, be broadband, extending from the ultraviolet (UV) to the near-infrared (NIR) region. In other words, plasmon nanofocusing has the potential to generate a white nanolight source [26, 27], which we will discuss in more detail later. However, it is important to note that the plasmon coupler may itself exhibit wavelength-dependent coupling efficiency, resulting in the confinement of a single wavelength that efficiently couples at the plasmon coupler.

2 | Fundamental Principles of Plasmon Nanofocusing

The standard tapered metallic structure used for plasmon nanofocusing in early research was primarily a solid conical gold tip [17, 28, 29]. Under ambient conditions, it can be seen as a tapered plasmonic waveguide in an insulator–metal–insulator setup, since it is surrounded by air, which acts as the insulator. In this setup, SPP waves propagate along the boundary between the metal and air, which is the surface of the conical gold tip. An electromagnetic wave is associated with a wavevector $k = n\,\omega/c$, where ω is the angular frequency, c is the speed of light, and n is the effective refractive index of the material for the propagating wave. In general, as the wavevector k increases, the wave confinement becomes more pronounced. The x, y, and z components of the wavevector k are bound in magnitude by $k^2 = k_x^2 + k_y^2 + k_z^2 = n^2(\omega/c)^2 = 4\pi^2 n^2/\lambda^2$, with λ being the wavelength. However, for SPPs, one component of k can be imaginary, allowing the other components to increase arbitrarily and, at the same time, providing subwavelength confinement to SPP waves. This allows metallic nanostructures to control and manipulate electromagnetic energy at subwavelength scales, with SPPs propagating along the metal surface at a wavelength much shorter and a wavevector much larger than that of far-field light. Because of

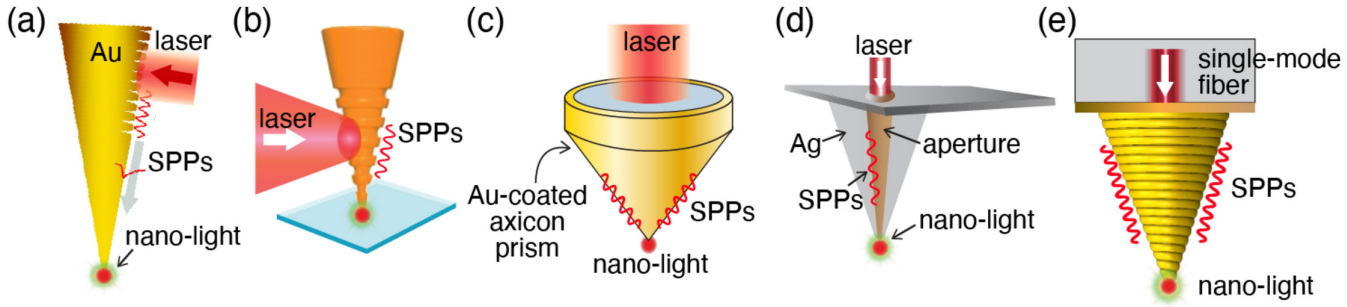

FIGURE 2 | Various types of plasmon coupling schemes used by researchers. (a) grating-type coupler on a solid conical gold tip [28], (b) solid conical gold tip with surface corrugated gratings [49], (c) axicon prism-based couplers [50], (d) aperture-based couplers in silver apertured conical tip [51], and (e) 3D printed corrugated tip with fiber coupler [52].

their evanescent nature, SPP waves do not propagate or radiate in the direction of the imaginary k and remain confined to the surface. The effective refractive index of a plasmonic material, which depends on the wavelength, can greatly surpass that of any naturally occurring material and increases further as the plasmonic structure gets smaller, such as toward the apex of the conical gold tip. A higher effective refractive index near the apex results in a larger wavevector, which further confines and slows down SPP waves. Therefore, in a tapered metallic nanostructure, including a conical gold tip, as the cross-sectional radius decreases along the propagation direction, it results in a continuous increase in the effective refractive index experienced by the SPP mode. This process can be understood by considering the taper as a sequence of infinitesimal cylindrical waveguides [30] with decreasing diameter and, therefore, increasing effective refractive index. Numerical solutions to Maxwell's equations for such a geometry confirm that the continuous gradient in the effective refractive index gradually reduces the group velocity, compressing the plasmon mode, concentrating electromagnetic energy, and enhancing the field strength at the apex [31, 32]. From a quantum perspective, the nanofocused field at the apex can be viewed as a coherent superposition of many plasmon modes that constructively interfere at the apex. Both classical and quantum considerations reveal that a tapered plasmonic material would nanofocus propagating SPPs into a nanometric volume, where they gradually slow down and concentrate electromagnetic energy as they propagate toward the apex. This leads to a significant field enhancement and tight confinement, provided the SPPs are effectively excited in the material.

Theoretically proposed for the first time by Nerkararyan in 1997 [33] and subsequently investigated in depth by Stockman in 2004 [25], plasmon nanofocusing has emerged as a compelling alternative technique for nanoconfining light fields, particularly following its first experimental demonstration by Raschke et al. in 2007 [28]. Since then, its applications have expanded to include optical nano-imaging [34–36] and nanoscale Raman spectroscopy [29, 37]. Furthermore, plasmon nanofocusing has also been demonstrated for nonlinear nano-optical phenomena, such as femtosecond time-resolved spectroscopy [38] and second-harmonic generation [39].

The key to achieving efficient plasmon nanofocusing lies in designing the tapered plasmonic nanostructures that exhibit smooth plasmon propagation, as well as an effective plasmon coupler to facilitate efficient energy transfer from propagating light to localized plasmons. Conical metal tips, typically fabricated by electrochemically etching gold nanowires (Figure 1b), have been commonly adopted for plasmon nanofocusing [16]. Other structures used for plasmon nanofocusing include silver-coated silicon dioxide pyramidal nanotips [40], tapered silver nanowedges [41], thin-film waveguide probes [42], plasmonic fiber tips [43–45], and a thin-film silicon waveguide with gradient thickness [46]. For efficient energy transfer, while grating-type plasmon couplers have been widely used (Figure 1c) [17, 28, 40], nanocrystal-based couplers [47, 48], solid conical gold tips with surface corrugated gratings [49], axicon prism-based couplers [50], aperture-based couplers [51], and 3D printed corrugated tips with fiber couplers [52] have also been reported. Figure 2 illustrates various types of plasmon couplers commonly used by researchers.

2.1 | The Choice of Plasmonic Material and Its Dimensions

To facilitate SPP waves as a collective surface charge density oscillation, the real part of the dielectric function of the plasmonic material must invert its sign at the interface. This criterion is easily met by metals such as gold or silver at optical frequencies. At other frequencies, alternative materials could be more suitable, such as aluminum in the blue and ultraviolet regions and tungsten in the IR region [53]. Therefore, selecting the right plasmonic metal is crucial for effectively facilitating SPP waves. Gold has been frequently employed as a material for conical tapered structures since it can be readily fabricated by elongating and sharpening a gold wire through an electrochemical etching process [54, 55]. Although this fabrication technique is well-established for producing gold conical tips with smooth surfaces, which are essential for efficient SPP propagation, it is not suitable for other plasmonic materials, such as silver and aluminum. When sharpened using a similar process, the surfaces of silver and aluminum wires become roughened due to chemical reactions. Although these materials are anticipated to yield superior results in plasmon resonance applications [56, 57], their surface roughness diminishes the efficiency of SPP propagation. Consequently, plasmon nanofocusing-based optical imaging has predominantly been conducted within longer wavelength ranges, such as the NIR region, where gold is preferred as a plasmonic material due to its lower ohmic losses, rather than in the visible or ultraviolet regions, where silver or aluminum would be more suitable [53, 58]. Additionally, most metals, unfortunately,

suffer from significant optical losses attributed to the positive imaginary component of their dielectric function. This phenomenon constrains the propagation of SPP waves, impacting practical applications in nanofocusing and light confinement. Therefore, it is crucial not only to choose the right type of metal but also to optimize the size of the plasmonic structure. Furthermore, the taper angle of the plasmonic structure is also significant. The adiabatic compression of energy during SPP propagation ensures minimal reflections and scattering losses, allowing efficient energy transfer to the nanoscale apex. When the taper angle stays below a certain threshold, the transformation is smooth enough to maintain mode continuity. As a result, the plasmon mode at the apex of the taper is fully converted into a highly localized mode with extreme spatial confinement [59]. Therefore, besides the type of metal and the dimensions of the metallic structure, the taper angle is also a crucial factor in enhancing the efficiency of plasmon nanofocusing. Generally, the smaller the taper angle, the greater the confinement. However, a small taper angle causes SPPs to propagate longer distances to reach the apex, increasing optical losses. At the same time, the taper angle is also practically limited by fabrication techniques.

2.2 | Plasmon Coupling Strategies

Efficiently launching SPPs onto a tapered metallic waveguide is a key factor for achieving high-intensity nanofocusing at the apex. Conservation of momentum is a necessary requirement for any kind of energy transfer between incident light and the SPPs. Direct far-field illumination of the tapered structure is inefficient because of the large momentum mismatch between far-field incident photons and SPPs. Therefore, a specialized coupling scheme is necessary to address this momentum mismatch. Although there are several possible ways to address this momentum mismatch, a well-designed grating fabricated at the shaft of the tip, away from the apex, has been commonly used as a plasmon coupler because it can be easily fabricated using focused ion beam (FIB) milling and provides reasonably good coupling efficiency. When illuminated with far-field propagating light, the grating coupler can scatter incident photons into propagating SPPs by providing the necessary in-plane momentum through adjusting the grating parameters and incident angle to compensate for the momentum mismatch between the incident light and SPPs. This scheme facilitates the smooth transfer of energy from incident photons to SPPs. The grating parameters are chosen to satisfy the phase-matching condition:

$$k_{SPP} = k_0 \sin\theta + m\,(2\pi / \Lambda), \tag{1}$$

where k_{SPP} is the plasmon wavevector, k_0 is the free-space wavevector, θ is the incidence angle, m is the diffraction order, and Λ is the grating period. By optimizing the grating parameters and the incident angle, the coupling efficiency of the grating-type plasmon coupler can be maximized for a given k_0, or the corresponding incident wavelength. This method also enables spatial separation between the coupling region and the apex, minimizing the leakage of far-field light toward the apex so that the incident light does not directly illuminate the sample near the apex. It is worth noting that since the phase-matching condition in Equation (1) depends on the incident wavelength (or on k_0), a particular grating will efficiently couple only one particular wavelength that satisfies the phase-matching condition. As mentioned earlier, in addition to the grating-type plasmonic couplers, aperture-based, nanocrystal-based, and axicon prism-based couplers have also been reported, where the phase-matching condition must also be satisfied.

3 | Plasmon Nanofocusing With Solid Conical Nanotips

Raschke's group experimentally demonstrated the phenomenon of plasmon nanofocusing for the first time in 2007 [28]. They used a solid conical tip made by electrochemically etching a gold nanowire, followed by the fabrication of a FIB-milled grating structure on the tip shaft several micrometers away from the apex [28, 29]. The radius of the tip apex was ~ 20 nm, and the cone angle was 15°. The grating periodicity of 750 nm efficiently launched SPPs when the grating coupler was illuminated with an incident wavelength of 765 nm, and the SPPs propagated over a distance exceeding 10 μm to the tip apex, generating a confined nanolight source at the apex (Figure 3a). The tip apex also functions as an optical antenna that radiates or scatters the nanofocused near-field light into

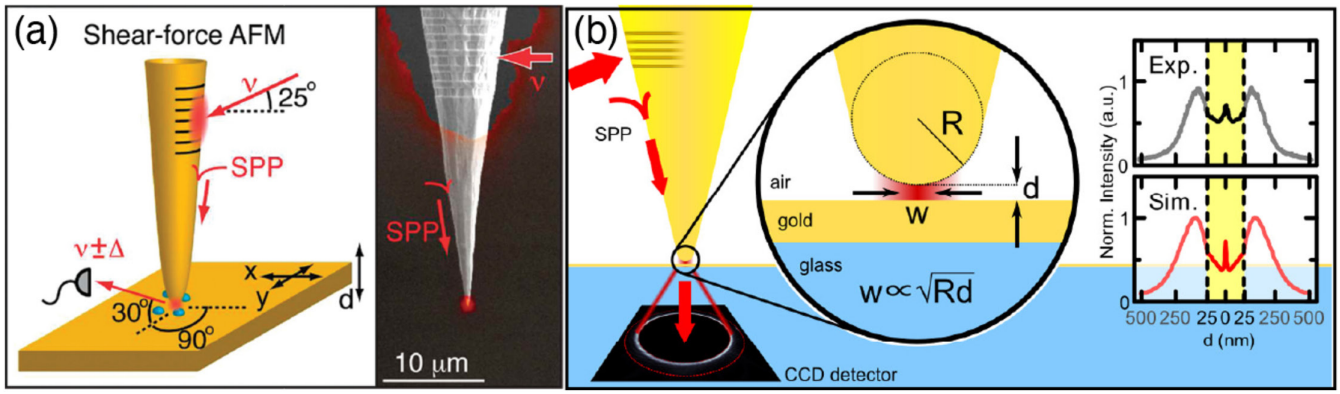

FIGURE 3 | (a) A schematic and an SEM image of an electrochemically etched Au tip with a grating fabricated using FIB. Incident light is focused onto the grating, and the Raman scattered light is excited by the nanofocused SPPs at the apex. The SEM image of the tip is overlaid with optical images of grating illumination and apex emission [29]. (b) A schematic of a gap-mode plasmon nanofocusing scheme where strong enhancement can be observed at small tip-sample separation, shown theoretically by the red curve and experimentally by the black curve [17].

the far field, making it easily measurable by conventional optics. The nanofocusing of the electromagnetic energy in the process of plasmon nanofocusing was demonstrated by imaging the scattering from the tip apex. For optimal grating excitation, the scattered light from the tip apex was intense yet confined to nanometer dimensions, in contrast to direct apex illumination, which resulted in weak and less localized emission.

Furthermore, a spectroscopic analysis revealed that the scattering from the apex was spectrally tunable, depending strongly on the incident angle and excitation wavelength, consistent with SPPs' dispersion relations and phase-matching conditions. A supporting discrete dipole numerical model also qualitatively matched the experimental data, indicating up to 10% conversion efficiency from the incident far-field light into propagating SPPs. However, because of propagation and ohmic losses, the scattered light power from the tip apex was estimated to be 0.1%–1% of the incident light, which can be considered significant given that the scattering occurs from a nanoscale light source. Considering the in-plane components of the wavevectors, optimal photon–plasmon coupling occurs when the incident light is polarized perpendicular to the groove orientation. When the polarization is parallel, no coupling is expected. The authors reported a strong dependence of the scattered light intensity from the tip apex on the polarization of the incident light. The efficiency of SPPs' propagation and resultant localization further depended on the smoothness of the tip-shaft between the grating and apex, as surface roughness and other defects acted as scattering centers that reduced nanofocusing performance.

While the authors did not conduct near-field optical experiments to directly characterize the field distribution at the tip apex, their results experimentally validated the process of plasmon nanofocusing, indicating that such nanofabricated tips could serve as bright nanolight sources, potentially applicable in aperture-less nanoscale microscopy and spectroscopy. Later, in 2010, the same group demonstrated TERS measurements utilizing plasmon nanofocusing, where a similar tip with an apex radius of about 10 nm was used [34]. The tip was operated with a shear-force atomic force microscope, and the grating coupler was illuminated at an incident angle of 25° in the side-illumination configuration. The authors compared TERS measurements taken in a traditional setup, where the tip apex is illuminated directly by incident light, with those obtained by employing plasmon nanofocusing to remotely illuminate the sample using a grating-type plasmon coupler, with dramatically reduced background for the latter. The authors suggested this technique would be especially useful for the study of bulk crystalline and biological samples, where conventional methods are hampered by strong background signals. In another study [29], the authors utilized NIR illumination and performed TERS imaging through plasmon nanofocusing. By scanning the tip across a nanoscale silicon step edge, the authors probed the extent of the near-field localization. The optical signal exhibited a spatial resolution of 22 ± 5 nm, which, after deconvolution, corresponded to an emission source confined to the 10-nm apex radius. This level of confinement was unattainable via direct illumination of the tip apex, and comparative measurements showed the background from direct illumination overwhelmed any edge-specific signal, illustrating the superiority of the nanofocusing approach with background suppression. Interestingly, the authors showed a predominantly axial (longitudinal) dipolar characteristic through the polarization analysis of the apex emission, confirming effective SPPs mode filtering during propagation, with only the radially symmetric TM mode contributing to the enhanced local field. They noted that asymmetries in SPPs excitation caused by side-illumination do not weaken the radial symmetry of the nanofocused mode at the apex, emphasizing the robustness of the conical geometry of the tip.

A related comprehensive theoretical study of mode evolution during plasmon nanofocusing was reported by Lu et al., who considered a conical silver tip with a grating-type plasmon coupler [60]. Using guided-wave theory, they derived eigenvalue equations for supported SPP modes on cylindrical metallic waveguides and showed that such structures support only TM and HE modes, with higher-order modes sequentially cut off as the radius decreases. Eventually, the TM mode persists and evolves toward the apex, where it transforms into a strongly localized mode, producing nanofocusing. Numerical simulations confirmed that excited SPPs launched by a grating coupler progressively converted through HE and TM modes before concentrating into a 20-nm radius apex through the TM mode. By revealing the stepwise mode evolution and identifying the surviving TM mode as the key channel for nanofocusing, this work provided mechanistic clarity to a phenomenon previously observed experimentally but not fully understood.

Becker et al. went one step further by involving gap-mode confinement to plasmon nanofocusing and investigated how coupling nanofocused plasmons with gap plasmons can drastically improve near-field confinement in NSOM [17]. Although previous reports confirmed that plasmon nanofocusing on a conical tip can achieve a spatial confinement of ~ 10 nm, probing single quantum emitters requires even smaller interaction volumes. Gap plasmons, which arise in nanometer-scale cavities between a metallic film and a tip apex, offer a solution by further squeezing fields beyond the apex radius. The authors experimentally approached an electrochemically etched gold tip (apex radius ~ 10 nm) toward a thin gold film (~ 30 nm) and detected transmitted light in *k*-space. A grating-type coupler optimized for an incident wavelength of 800 nm was milled into the taper shaft by FIB milling. As the tip-sample distance decreased, a sharp increase in scattering intensity was observed (Figure 3b). This signal, absent at larger distances, was identified as the signature of gap plasmons. When the tip apex approaches the metal film, the nanofocused field hybridizes with film-supported SPPs, forming highly confined gap plasmons. These gap modes significantly increase local field intensity, enabling excitation volumes smaller than 10 nm and tunable down to a few nanometers. This controlled generation of gap plasmons establishes a robust method for nanospectroscopy at single-molecule scales.

4 | Plasmon Nanofocusing on Metal-Coated Dielectric Nanotips

Solid metallic conical tips, typically fabricated through electrochemical etching of metallic nanowires, suffer from restricted material choices (mostly gold), limited shape control, and challenges in tuning plasmonic properties for various experimental

conditions. These constraints arise from the limitations inherent in the electrochemical growth process and its practical applicability; as such, these tips can only be handled with either a scanning tunneling microscope (STM) or a tuning-fork-based shear-mode AFM. Such limitations hinder reproducibility, constrain applications to narrow wavelength ranges, and restrict practical applications. In 2016, Umakoshi et al. introduced an innovative plasmonic tip design that addresses these longstanding challenges in plasmon nanofocusing [40]. Their design features a flexible structure comprising a dielectric pyramidal body coated with a thin metallic layer on one face of the pyramidal structure, combined with a grating-type plasmon coupler fabricated by FIB-milling away from the apex (Figure 4a). A numerically calculated field distribution near the apex is shown in Figure 4b. The base of the tip was a pyramidal AFM cantilever, which is available in various dielectric materials, including silicon, silicon nitride, and doped semiconductors. In addition, these base materials can be partially or fully oxidized to precisely tune their dielectric constants. A thin metallic layer was deposited onto the chosen base material using a carefully controlled thermal evaporation technique that achieves ultra-low surface roughness while permitting the selection of any desired metal for evaporation. The pyramidal shape of the tip facilitates selective evaporation on one of its flat, tapered surfaces, ensuring a uniform thickness of the metallic layer in a tapered wedge shape. This architecture enables the independent tuning of the dielectric substrate, metal type, and metal thickness, allowing for precise control over plasmon propagation and nanofocusing. Using finite-difference time-domain (FDTD) simulations, the authors evaluated the performance of tips with diverse material combinations. For excitation at 642 nm, a silver metallic layer on a silicon dioxide body was identified as optimal, generating near-field intensities several orders of magnitude higher than those of gold-coated tips. The choice of dielectric substrate was also shown to be critical, as silicon dioxide minimized losses, whereas silicon significantly suppressed the near-field intensity by nearly two orders of magnitude.

Experimentally, the authors selected commercially available pyramidal silicon AFM cantilever tips, the base material of which was fully oxidized at a high temperature in the presence of water vapor, followed by deposition of smooth metallic coatings on one face of these oxidized tips via optimized thermal evaporation, achieving atomically flat surfaces (<1 nm roughness). This smoothness allowed reliable propagation of plasmons without scattering losses. Gratings were patterned using FIB milling with numerically optimized parameters to efficiently couple incident photons and SPPs. Figure 4c shows an SEM image of the fabricated tip. Near-field imaging experiments demonstrated nearly 100% reproducibility in plasmon nanofocusing [40], representing a significant advance over the inconsistent performance of electrochemically etched tips. A strong dependence on the polarization of the incident light was observed, with polarization perpendicular to the groove direction providing the best coupling and polarization parallel to the groove direction resulting in no coupling and, consequently, no confined near-field light at the apex (Figure 4d,e). The authors measured the near-field image of a carbon nanotube (CNT) bundle, demonstrating that the image could only be obtained when the incident polarization was set perpendicular to the groove direction, and

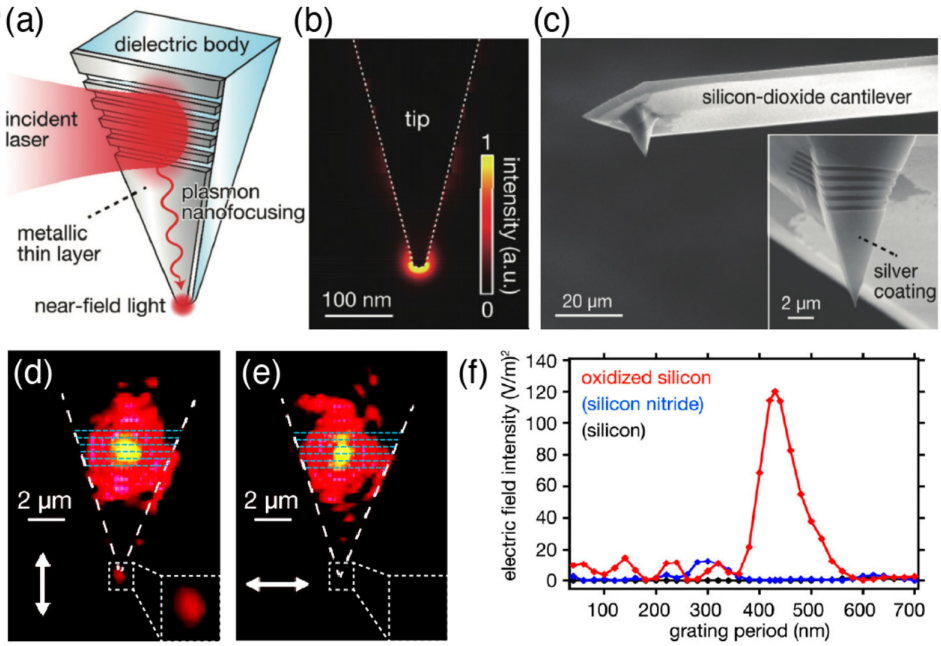

FIGURE 4 | (a) Schematic of a tip structure featuring a dielectric pyramidal structure with a metallic thin layer on one side, along with a grating-type plasmon coupler. (b) An intensity map of the electric field near the tip apex, simulated using FDTD. (c) SEM image of a fabricated tip, with the inset showing a zoomed-in view of the tip to highlight the grating structure. (d, e) Optical images of a fabricated tip illuminated by a laser at the grating, with incident polarizations indicated by white arrows. The white dotted lines represent the outer shapes of the tips and gratings. Insets show magnified images of the apex. For the polarization perpendicular to the grating grooves in (d), a bright spot appears at the apex, while the light spot disappears in (e), where the polarization is parallel to the grating [40]. (f) FDTD simulation showing the relationship between the near-field light intensity at the tip apex and the grating period, confirming that the oxidized silicon tip provides about 10 times stronger near-field intensity than the silicon nitride tip and 63 times stronger near-field intensity than the silicon tip [61].

no scattering from the CNT sample was observed when the incident polarization was aligned parallel to the groove direction.

This innovative design also offered crucial practical benefits. For instance, it enabled the free selection of both the base material and the metal, making it easier to achieve atomically flat surfaces for any chosen metal to improve control over plasmon propagation and reduce surface scattering. This is in contrast to electrochemically etched tips, which had strict restrictions on metal choice and resulted in poor surface smoothness. Because only one side of the pyramidal tip was metal-coated, plasmon propagation was directionally confined to one surface as it propagated toward the apex, thereby reducing propagation losses and maximizing energy concentration. The planar coating surface facilitated the use of established FIB-milling techniques for fabricating grating couplers with uniform depths and other parameters, which is not easy on a curved surface, such as on a conical body. Moreover, since the tip was based on AFM cantilevers, it was compatible with widely used optical lever feedback systems, unlike electrochemically etched tips, which are restricted to tuning fork or STM-based NSOM setups, limiting the samples that can be investigated with such a solid conical tip. The authors highlighted their design as highly efficient, reliable, and adaptable, as it provided flexibility in both materials and geometry, which facilitated customization for various excitation wavelengths and sample categories. The demonstration of nearly 100% reproducibility represents a significant milestone for practical NSOM applications, including nano-Raman spectroscopy, TERS nanoimaging, optical sensing, and ultrahigh-resolution bioimaging.

In another study conducted by the same research group, Yadav et al. demonstrated the application of plasmon nanofocusing in the context of photoluminescence, utilizing a similar pyramidal cantilever-based silver-coated tip [62]. The authors tackled a major issue of photodegradation of samples during extended illumination in fluorescence nanoimaging, which can be a substantial concern for various chemical and biological samples. In conventional NSOM-based fluorescence measurements, the plasmonic tip is directly illuminated at the apex to excite fluorescence from a nanoscale region of the sample. However, this approach inadvertently exposes a larger sample area within the diffraction-limited focal spot of the incident beam, leading to severe photo-induced damage and degradation of the fluorescence signal within the focal spot. The authors demonstrated that this issue could be overcome by spatially separating the excitation site from the illumination source via plasmon nanofocusing. The experimental design involved fabricating silver-coated tips on oxidized silicon pyramidal cantilevers, with smooth metallic films deposited through thermal evaporation, followed by the fabrication of a grating coupler via FIB milling, several micrometers away from the tip apex. A Nile blue sample was illuminated with an incident wavelength of 642 nm, which was a suitable choice of incident energy for inducing photoluminescence within the sample. Compared to conventional NSOM, the fluorescence signals obtained via NSOM based on plasmon nanofocusing preserved their intensity and spectral integrity over prolonged exposure durations, underscoring the robustness of this technique for extended measurements. On the other hand, the fluorescence intensity was observed to diminish dramatically and rapidly in the focal area during the raster scanning when measured using traditional NSOM, where the tip apex was directly illuminated by the laser. This research demonstrates that plasmon nanofocusing not only enhances spatial resolution but also preserves sample quality by reducing photodamage, a crucial consideration for sensitive samples, such as biological or chemical molecules and nanomaterials.

To gain a deeper understanding of the experimental results and identify the optimal parameters for the experiment, the same group later provided a detailed numerical analysis of the optical properties of a similar tapered tip fabricated on a pyramidal base [61]. In their FDTD simulation study, the authors investigated how various structural parameters, including the dielectric material of the base, the thickness of the metallic film, and the apex angle, influence the near-field intensity and confinement at the tip apex. For silver-coated tips, they assessed the near-field distribution for bases made of silicon, silicon nitride, and oxidized silicon. The results showed that oxidized silicon provides the most effective dielectric support for efficient plasmon nanofocusing, minimizing losses and enhancing field intensity (Figure 4f). Similarly, the thickness of the metallic layer was found to be crucial. Thinner layers suppressed plasmon propagation due to poor confinement and crosstalk between plasmons on opposite sides of the silver film, whereas excessively thick coatings increased damping losses and reduced confinement because of a thicker apex. An optimal silver thickness of around 40 nm produced the best nanofocusing. Additionally, the authors established that the apex angle significantly influences nanofocusing, with sharper angles allowing for tighter confinement; however, careful optimization is necessary for practical fabrication due to the limitations of the FIB milling process. The analysis also confirmed that the designed structure supports stable plasmon propagation over several micrometers with minimal losses, creating a highly localized nanolight at a 20-nm apex. The study highlights the importance of material and geometric tuning for effective and consistent plasmon nanofocusing, especially in applications like NSOM and TERS. It also lays the groundwork for adapting the pyramidal cantilever-based tip design to a range of nanoscale optical applications, including Raman spectroscopy, nanoimaging, and single-molecule detection.

5 | Broadband Plasmon Nanofocusing and White Nanolight Source

As a technique based on plasmon propagation, plasmon nanofocusing is inherently wavelength-independent, unlike plasmon-resonance-based techniques, where resonant enhancement occurs only within a very narrow wavelength range near the resonance wavelength. Therefore, plasmon nanofocusing is expected to be a broadband phenomenon. However, while the process of plasmon nanofocusing itself does not depend on wavelength, launching SPPs at the plasmon coupler can be highly wavelength-dependent, which makes the confined light at the tip apex wavelength-dependent. The phase-matching condition at the plasmon coupler, as dictated by momentum conservation and shown in Equation (1), involves the free-space wavevector of the incident light, k_0, which determines the grating parameters for a grating-type plasmon coupler. Different incident wavelengths, or different values of k_0, require gratings with different parameters. This means that a particular grating will efficiently

couple only one specific wavelength, making the entire process wavelength-dependent. But what happens when a plasmon coupler is created by superimposing multiple gratings, each suitable for coupling a different wavelength within a broadband spectrum? One would expect such a coupler to efficiently couple the superposition of all wavelengths within that broadband spectrum. Once efficiently coupled, the subsequent process of propagation and adiabatic compression would be wavelength-independent, allowing all coupled wavelengths within the bandwidth to nanofocus and coexist at the apex, thus creating a white nanolight source at the apex. Light with a single wavelength is a sinusoidal wave, and the corresponding plasmon coupler is a grating, both having specific periods. A grating with a particular period can couple plasmons to light with a matching period, as determined by the phase-matching condition. White light can be considered as a combination of multiple wavelengths, and a superposition of these wavelengths forms a pulse wave function (Figure 5a). Similarly, the superposition of gratings with different periods would resemble a structure similar to a single slit. Thus, a single slit is expected to serve as an effective coupler for broadband incident light, as shown in Figure 5b. It is also worth noting that propagation-related energy losses can slightly depend on wavelength, leading to minor intensity variations among different wavelength components in the confined white nanolight at the apex, although it would contain all possible wavelengths present in the incident light.

Umakoshi et al. recently reported the first experimental demonstration of a broadband white nanolight source created through plasmon nanofocusing spanning over the entire visible spectrum and even extending into the NIR region [26]. In their study, the authors employed a single slit as a plasmon coupler for white incident light. They discovered, through both numerical simulation and their experiment, that a single slit of 200 nm, fabricated ~ 8 μm away from the apex on a 40-nm-thick silver-coated pyramidal silicon dioxide tip, was most effective for coupling light across the entire visible range. While the authors confirmed strong near-field confinement at the tip apex for wavelengths ranging from 400 to 1200 nm in FDTD simulations, their experimental demonstration was limited to the visible and extending slightly into the NIR region due to experimental constraints (Figure 5c). Visual observation of the light scattered from the tip apex through various color filters revealed the presence of multiple wavelengths (Figure 5d). Experimental optical imaging through bandpass filters, as well as spectrally resolved scattering measurements, also verified that a single tip provided strong, localized near-field light spanning the entire visible range, and even into the NIR. The authors demonstrated nanoscale spectral imaging of CNTs, successfully mapping their electronic bandgap transitions with high spatial resolution. Unlike resonance-based NSOM approaches, which can only analyze a single electronic transition or bandgap, the white nanolight source produced through broadband plasmon nanofocusing allows for the spatial mapping of multiple absorption and scattering features in a single scan. Distinct bandgap energies were clearly visualized, confirming the ability of the white nanolight to probe multiple optical transitions in a single experiment.

This scheme eliminates the need for lock-in detection due to background suppression, is free of chromatic aberration since all wavelengths are compressed to the same nanometric spot, and can be adapted for any desired wavelength range with appropriate design. The white nanolight source created through plasmon nanofocusing facilitates multicolor near-field imaging, multiband Raman spectroscopy, nonlinear optics, and broadband near-field sensing and trapping, providing a universal, high-performance tool for nanophotonics research. It offers a reliable and reproducible method for producing versatile, broadband nanolight sources, with applications extending across materials science, spectroscopy, and biology.

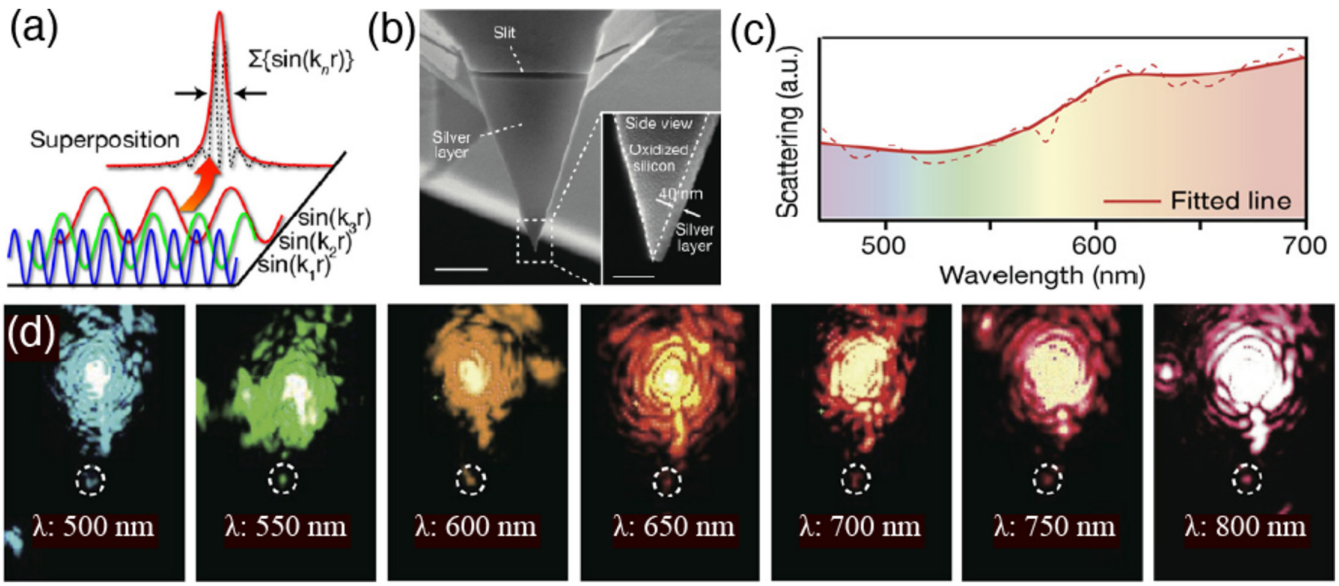

FIGURE 5 | (a) Schematic of plasmon nanofocusing for white light using a single-slit coupler. (b) Superposition of sine waves with different wave vectors, creating a pulsed-shaped structure. (c) SEM image of the fabricated tapered silver structure with a single-slit coupler. The inset shows a side view of the silver layer. (d) Scattering spectrum of the optical spot at the apex, demonstrating white-light characteristics. (e) Optical images of the tapered silver structure illuminated with a supercontinuum laser, observed through a series of band-pass filters indicated by their central wavelengths [26].

An in-depth theoretical investigation of broadband plasmon nanofocusing using FDTD simulations was also reported by the same group [41], where the authors explored the broadband capabilities based on plasmonic materials and various parameters of the tapered structure. In this study, instead of using a self-standing tip, the authors employed two-dimensional wedge-shaped metallic tapers fabricated on glass substrates, together with a single-slit-type plasmon coupler fabricated several micrometers away from the wedge apex, to systematically study broadband excitation (Figure 6a). Such a system cannot be used for scanning and nanoimaging; however, it has many other interesting applications, including multimodal nanospectroscopy, nanosensing, nanotrapping, and optical nanoswitching. Simulations demonstrated that plasmon nanofocusing can confine light across the entire visible spectrum, extending into the near-UV and NIR regions (350–1800 nm).

Authors systematically compare different plasmonic materials (aluminum, silver, and gold) and geometrical parameters (metal thickness, taper angle, and slit width) to investigate not only the optimum nanofocusing but also the broadband capabilities. They found that material choice significantly influenced spectral coverage, as silver excelled in the visible range, gold extended into the NIR, and aluminum covered shorter wavelengths. Aluminum tapers produced the broadest spectral range

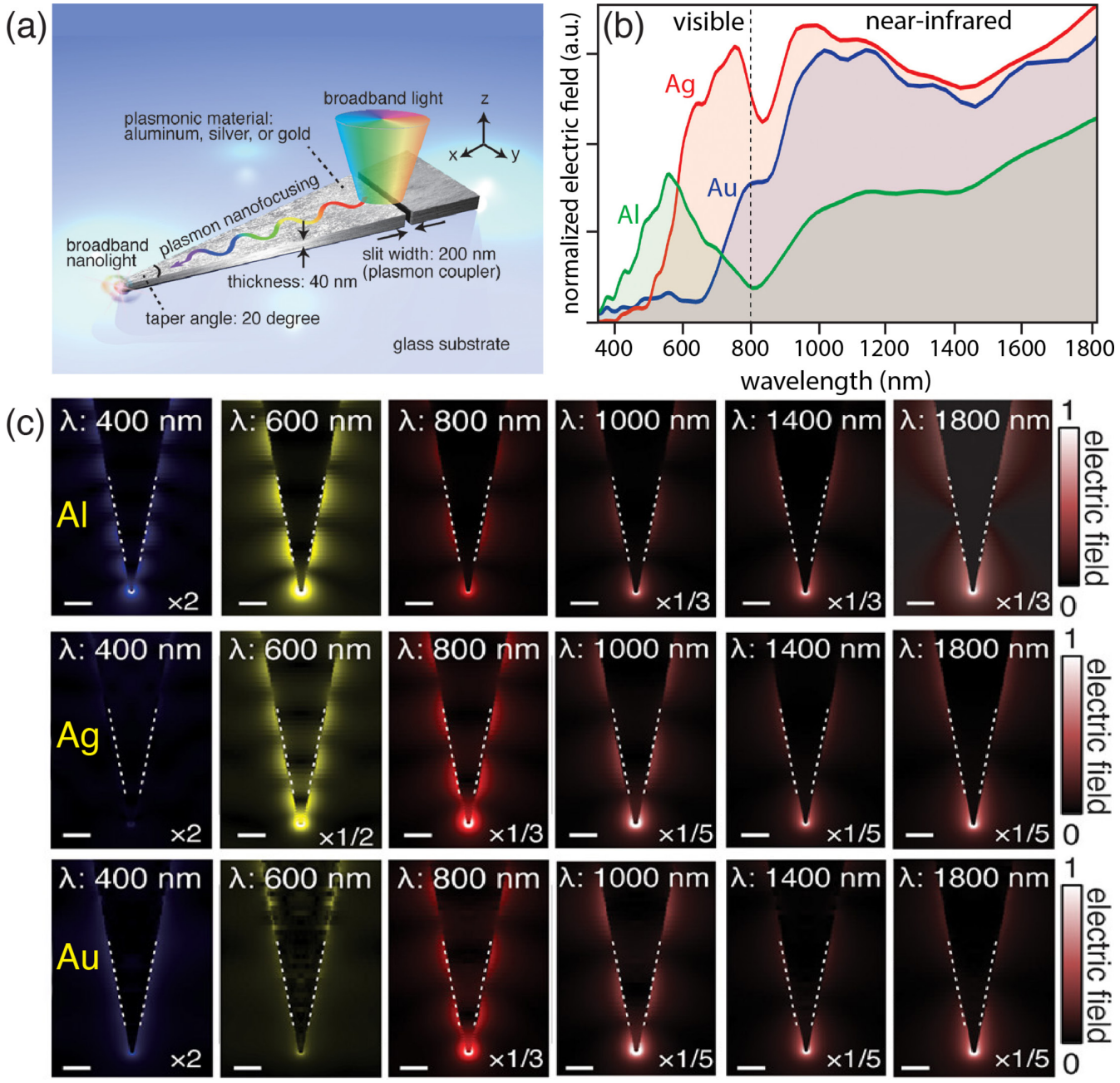

FIGURE 6 | (a) Schematic illustration of a 2D metallic tapered structure, with a single-slit coupler, on a glass substrate. (b) Electric field strength in the near-field spectra at taper apexes for aluminum, silver, and gold materials, normalized by the incident light spectrum. (c) Electric field distributions near the apex for aluminum, silver, and gold at different wavelengths [41].

(350–1800 nm), including the near-UV range, owing to its favorable dielectric properties at shorter wavelengths. Silver operated effectively from ~ 500 nm, and gold, limited by interband transitions, from ~ 700 nm onward (Figure 6b). Silver achieved the highest field intensity in the NIR, though gold is superior for stability in real-world applications. Figure 6c shows electric field distributions near the apex for aluminum (upper panel), silver (middle panel), and gold (lower panel) tapered structures at different incident wavelengths, confirming the generation of confined light at the apex for all materials across a wide wavelength range. The authors reported that the thickness of the metallic wedge also significantly influences its broadband capabilities. Thicker metallic layers (> 40 nm) reduce near-field intensity, especially in the NIR, due to greater plasmonic mode volume and weaker confinement. At the same time, thin films (< 20 nm) experience cross-surface plasmon coupling, which can undermine broadband performance, particularly at short wavelengths. A thickness of approximately 40 nm was found to be optimal. The taper angle and slit width had only a modest influence on near-field intensity and nanofocusing efficiency. Spectral broadness also remained reasonably robust across slight variations in the taper angles and slit width.

Following their numerical optimizations, the authors proceeded to conduct experiments by fabricating wedge-shaped two-dimensional tapers on glass substrates. They deposited 40-nm-thick metal layers (gold, silver, and aluminum) via thermal evaporation then used FIB lithography to fabricate the wedge-shaped tapers with specific apex angles and single-slit-type plasmon couplers. The plasmon couplers on the tapers were illuminated with white light, and the scattered light at the apex, where nanofocused near-field light radiates into the far-field, was observed. The experimental results confirmed high-fidelity broadband nanofocusing, with detectable near-field light at the apex across the visible spectrum for all three metals. However, due to experimental limitations, only the visible range was examined. The authors found that while aluminum covered the entire visible spectrum, silver performed best at wavelengths longer than 500 nm and gold at wavelengths longer than 700 nm. These findings strongly supported the simulation results. Importantly, the spatial profile of the localized light remained consistent across the spectrum, indicating that all wavelengths focused into the same nanometric volume, in contrast to higher-order plasmonic resonance modes.

6 | Conclusions

Plasmon nanofocusing has revolutionized the way we perceive traditional optical nanoscopy techniques by enabling background-free, highly confined light at the nanoscale, overcoming the limitations of narrowband resonances. Both theoretical considerations and experimental results have shown how plasmon nanofocusing can be leveraged not only for high-contrast imaging but also for creating fundamentally new forms of light. It does so through adiabatic compression of propagating SPPs along tapered metallic structures, producing a phase-stable, background-free, and broadband nanolight source. When integrated into NSOM and TERS, it has the potential to push spatial resolution into the single-nanometer range due to the background-free observation, enabling single-molecule sensitivity and opening new possibilities for ultrafast nanoscale spectroscopy. Advances in coupling strategies, from grating-assisted excitation to single-slit excitation, have improved efficiency and expanded operational bandwidths across a wide spectral range from near-UV to NIR. Future applications could seamlessly extend to biological uses, where preventing photodegradation is especially critical for live-cell imaging. White nanolight sources could facilitate the simultaneous probing of multiple fluorophores. Broadband nanofocusing can also be used to drive multiwavelength nonlinear processes, such as four-wave mixing and harmonic generation, at the nanoscale, with high efficiency. It may further connect with quantum emitters across various wavelengths, offering significant implications for quantum photonics. Additionally, by systematically exploring different metals and dielectrics, nanofocusing could extend into the ultraviolet range for bio-labeling or into the midinfrared range for vibrational spectroscopy.

Despite these achievements, there is still room for improvement in the plasmon nanofocusing technique, including the fabrication of precision tapers for smoother plasmon propagation, optimization of plasmon couplers to improve coupling efficiency, mitigation of thermal effects, and protection of plasmonic tapers from degradation due to various factors during experiments, including atmospheric interactions. Future directions point toward the use of novel materials, quantum plasmonic applications, and on-chip integration, which could make nanofocusing a foundational technology in next-generation optical devices. As fabrication technologies mature and new materials are introduced, plasmon nanofocusing will continue to advance toward higher performance, stability, and broader applicability. Its impact is expected to extend well beyond Raman spectroscopy, influencing areas such as nonlinear nanooptics, nanoscale light–matter interactions, and integrated photonics. Looking forward, nanofocusing is poised to play a central role in quantum plasmonics, where single or entangled photons interact strongly with matter at the nanoscale. The combination of extreme confinement and coherent control could enable new quantum information processing schemes, nanoscale light sources, and sensors with unprecedented sensitivity.

Conflicts of Interest

The authors declare no conflicts of interest.

Data Availability Statement

The data that support the findings of this study are available on request from the corresponding author. The data are not publicly available due to privacy or ethical restrictions.

References

1. G. Xu, Z. Liu, K. Xu, et al., "Constant Current Etching of Gold Tips Suitable for Tip-Enhanced Raman Spectroscopy," *Review of Scientific Instruments* 83 (2012): 103708.

2. S. Kawata, Y. Inoue, and P. Verma, "Plasmonics for Near-Field Nano-Imaging and Superlensing," *Nature Photonics* 3 (2009): 388–394.

3. R. Bachelot, P. Gleyzes, and A. C. Boccara, "Reflection-Mode Scanning Near-Field Optical Microscopy Using an Apertureless Metallic Tip," *Applied Optics* 36 (1997): 2160–2170.

4. A. Lahrech, R. Bachelot, P. Gleyzes, and A. C. Boccara, "Infrared-Reflection-Mode Near-Field Microscopy Using an Apertureless Probe With a Resolution of λ/600," *Optics Letters* 21 (1996): 1315–1317.

5. P. Verma, "Tip-Enhanced Raman Spectroscopy: Technique and Recent Advances," *Chemical Reviews* 117 (2017): 6447–6466.

6. P. Verma, T. Ichimura, T. Yano, T. Saito, and S. Kawata, "Nano-Imaging Through Tip-Enhanced Raman Spectroscopy: Stepping Beyond the Classical Limits," *Laser & Photonics Reviews* 4 (2010): 548–561.

7. R. Zenobi, N. Kumar, and P. Verma, "Spatial Resolution in Nanoscale TERS Imaging: Current Status, Challenges, and Guidelines," *Nano Letters* 25 (2025): 3707–3716.

8. W. Zhang, B. S. Yeo, T. Schmid, and R. Zenobi, "Single Molecule Tip-Enhanced Raman Spectroscopy With Silver Tips," *Journal of Physical Chemistry C* 111 (2007): 1733–1738.

9. T. Mono, Y. Saito, and P. Verma, "Quantitative Analysis of Polarization-Controlled Tip-Enhanced Raman Imaging through the Evaluation of the Tip Dipole," *ACS Nano* 8 (2014): 10187.

10. A. Taguchi, J. Yu, P. Verma, and S. Kawata, "Optical Antennas With Multiple Plasmonic Nanoparticles for Tip-Enhanced Raman Microscopy," *Nanoscale* 7 (2015): 17424–17433.

11. T. W. Johnson, Z. J. Lapin, R. Beams, et al., "Highly Reproducible Near-Field Optical Imaging With Sub-20-nm Resolution Based on Template-Stripped Gold Pyramids," *ACS Nano* 6 (2012): 9168–9174.

12. T. L. Vasconcelos, B. S. Archanjo, B. S. Oliveira, et al., "Plasmon-Tunable Tip Pyramids: Monopole Nanoantennas for Near-Field Scanning Optical Microscopy," *Advanced Optical Materials* 6 (2018): 1800528.

13. R. M. Stöckle, Y. D. Suh, V. Deckert, and R. Zenobi, "Nanoscale Chemical Analysis by Tip-Enhanced Raman Spectroscopy," *Chemical Physics Letters* 318 (2000): 131–136.

14. M. S. Anderson, "Locally Enhanced Raman Spectroscopy With an Atomic Force Microscope," *Applied Physics Letters* 76 (2000): 3130–3132.

15. N. Hayazawa, Y. Inouye, Z. Sekkat, and S. Kawata, "Metallized Tip Amplification of Near-Field Raman Scattering," *Optics Communication* 183 (2000): 336.

16. L. G. Cançado, A. Hartschuh, and L. Novotny, "Tip-Enhanced Raman Spectroscopy of Carbon Nanotubes," *Journal of Raman Specroscopy* 40 (2009): 1420–1426.

17. S. F. Becker, M. Esmann, K. W. Yoo, et al., "Gap-Plasmon-Enhanced Nanofocusing Near-Field Microscopy," *ACS Photonics* 3 (2016): 223–232.

18. P. Groß, M. Esmann, S. F. Becker, J. Vogelsang, N. Talebi, and C. Lienau, "Plasmonic Nanofocusing – Grey Holes for Light," *Advances in Physics: X* 1 (2016): 297–330.

19. F. Lu, W. Zhang, M. Liu, L. Zhang, and T. Mei, "Tip-Based Plasmonic Nanofocusing: Vector Field Engineering and Background Elimination," *IEEE Journal of Selected Topics in Quantum Electronics* 27 (2021): 1–12.

20. R. Hillenbrand and F. Keilmann, "Complex Optical Constants on a Subwavelength Scale," *Physical Review Letters* 85 (2000): 3029–3032.

21. F. Zenhausern, M. P. O'Boyle, and H. K. Wickramasinghe, "Apertureless Near-Field Optical Microscope," *Applied Physics Letters* 65 (1994): 1623–1625.

22. J. Yu, Y. Saito, T. Ichimura, S. Kawata, and P. Verma, "Far-Field Free Tapping-Mode Tip-Enhanced Raman Microscopy," *Applied Physics Letters* 102 (2013): 123110.

23. B. Ranjan, Y. Saito, and P. Verma, "High-Sensitivity Pesticide Detection Using Particle-Enhanced Resonant Raman Scattering," *Applied Physics Express* 9 (2016): 032401.

24. I. Maouli, A. Taguchi, Y. Saito, S. Kawata, and P. Verma, "Optical Antennas for Tunable Enhancement in Tip-Enhanced Raman Spectroscopy Imaging," *Applied Physics Express* 8 (2015): 032401.

25. M. I. Stockman, "Nanofocusing of Optical Energy in Tapered Plasmonic Waveguides," *Physical Review Letters* 93 (2004): 137404.

26. T. Umakoshi, M. Tanaka, Y. Saito, and P. Verma, "White Nanolight Source for Optical Nanoimaging," *Science Advances* 6 (2020): eaba4179.

27. X. Ma, Q. Liu, N. Yu, et al., "6 nm Super-Resolution Optical Transmission and Scattering Spectroscopic Imaging of Carbon Nanotubes Using a Nanometer-Scale White Light Source," *Nature Communications* 12 (2021): 6868.

28. C. Ropers, C. C. Neacsu, T. Elsaesser, M. Albrecht, M. B. Raschke, and C. Lienau, "Grating-Coupling of Surface Plasmons Onto Metallic Tips: A Nanoconfined Light Source," *Nano Letters* 7 (2007): 2784–2788.

29. S. Berweger, J. M. Atkin, R. L. Olmon, and M. B. Raschke, "Adiabatic Tip-Plasmon Focusing for Nano-Raman Spectroscopy," *Journal of Physical Chemistry Letters* 1 (2010): 3427–3432.

30. L. Novotny and C. Hofner, "Light Propagation in a Cylindrical Waveguide With a Complex, Metallic, Dielectric Function," *Physical Review E* 50 (1994): 4094.

31. V. S. Gurevich and M. N. Libenson, "Surface Polaritons Propagation Along Micropipettes," *Ultramicroscopy* 57 (1995): 277–281.

32. A. J. Babadjanyan, N. L. Margaryan, and K. V. Nerkararyan, "Superfocusing of Surface Polaritons in the Conical Structure," *Journal of Applied Physics* 87 (2000): 3785–3788.

33. K. V. Nerkararyan, "Superfocusing of a Surface Polariton in a Wedge-Like Structure," *Physics Letters A* 237 (1997): 103–105.

34. C. C. Neacsu, S. Berweger, R. L. Olmon, L. V. Saraf, C. Ropers, and M. B. Raschke, "Near-Field Localization in Plasmonic Superfocusing: A Nanoemitter on a Tip," *Nano Letters* 10 (2010): 592–596.

35. D. Sadiq, J. Shirdel, J. S. Lee, E. Selishcheva, N. Park, and C. Lienau, "Adiabatic Nanofocusing Scattering-Type Optical Nanoscopy of Individual Gold Nanoparticles," *Nano Letters* 11 (2011): 1609–1613.

36. Z. Zhang, P. Ahn, B. Dong, O. Balogun, and C. Sun, "Quantitative Imaging of Rapidly Decaying Evanescent Fields Using Plasmonic Near-Field Scanning Optical Microscopy," *Scientific Reports* 3 (2013): 2803.

37. F. D. Angelis, G. Das, P. Candeloro, et al., "Nanoscale Chemical Mapping Using Three-Dimensional Adiabatic Compression of Surface Plasmon Polaritons," *Nature Nanotechnology* 5 (2010): 67–72.

38. V. Kravtsov, R. Ulbricht, J. M. Atkin, and M. B. Raschke, "Plasmonic Nanofocused Four-Wave Mixing for Femtosecond Near-Field Imaging," *Nature Nanotechnology* 11 (2016): 459–464.

39. S. Schmidt, B. Piglosiewicz, D. Sadiq, et al., "Adiabatic Nanofocusing on Ultrasmooth Single-Crystalline Gold Tapers Creates a 10-nm-Sized Light Source With Few-Cycle Time Resolution," *ACS Nano* 6 (2012): 6040–6048.

40. T. Umakoshi, Y. Saito, and P. Verma, "Highly Efficient Plasmonic Tip Design for Plasmon Nanofocusing in Near-Field Optical Microscopy," *Nanoscale* 8 (2016): 5634–5640.

41. K. Taguchi, T. Umakoshi, S. Inoue, and P. Verma, "Broadband Plasmon Nanofocusing: Comprehensive Study of Broadband Nanoscale Light Source," *Journal of Physical Chemistry C* 125 (2021): 6378–6386.

42. K. Zhang, Y. Bao, M. Cao, et al., "Low-Background Tip-Enhanced Raman Spectroscopy Enabled by a Plasmon Thin-Film Waveguide Probe," *Analytical Chemistry* 93 (2021): 7699–7706.

43. C. Meng, Z. Xie, F. Lu, et al., "Fiber Vector Light-Field-Based Tip-Enhanced Raman Spectroscopy," *Nano Letters* 25 (2025): 2112–2117.

44. F. Lu, W. Zhang, L. Zhang, et al., "Nanofocusing of Surface Plasmon Polaritons on Metal-Coated Fiber Tip Under Internal Excitation of Radial Vector Beam," *Plasmonics* 14 (2019): 1593–1599.

45. Z. Xie, C. Meng, D. Yue, L. Xu, T. Mei, and W. Zhang, "Tip-Enhanced Raman Scattering of Glucose Molecules," *Opto-Electronics Science* 4 (2025): 240027.

46. K. Zhang, S. Taniguchi, and T. Tachizaki, "Generation of Broadband Near-Field Optical Spots Using a Thin-Film Silicon Waveguide With Gradually Changing Thickness," *Optics Letters* 43 (2018): 5937–5940.

47. K. Sakai, T. Yamamoto, and K. Sasaki, "Nanofocusing of Structured Light for Quadrupolar Light-Matter Interactions," *Scientific Reports* 8 (2018): 7746.

48. Y. Fujita, P. Walke, S. D. Feyter, and H. Uji-I, "Remote Excitation-Tip-Enhanced Raman Scattering Microscopy Using Silver Nanowire," *Japanese Journal of Applied Physics* 55 (2016): 08NB03.

49. H. Shen, G. Lu, Y. He, Y. Cheng, H. Liu, and Q. Gong, "Directional and Enhanced Spontaneous Emission With a Corrugated Metal Probe," *Nanoscale* 6 (2014): 7512–7518.

50. K. Kato, A. Ono, W. Inami, and Y. Kawata, "Plasmonic Nanofocusing Using a Metal-Coated Axicon Prism," *Optics Express* 18 (2010): 13580–13585.

51. I.-Y. Park, S. Kim, J. Choi, et al., "Plasmonic Generation of Ultrashort Extreme-Ultraviolet Light Pulses," *Nature Photonics* 5 (2011): 677–681.

52. L. Long, Q. Deng, R. Huang, J. Li, and Z.-Y. Li, "3D Printing of Plasmonic Nanofocusing Tip Enabling High Resolution, High Throughput and High Contrast Optical Near-Field Imaging," *Light: Science & Applications* 12 (2023): 219.

53. C. Lindquist, P. Nagpal, K. M. McPeak, D. J. Norris, and S. H. Oh, "Engineering Metallic Nanostructures for Plasmonics and Nanophotonics," *Reports on Progress in Physics* 75 (2012): 036501.

54. X. Wang, Z. Liu, M.-D. Zhuang, et al., "Tip-Enhanced Raman Spectroscopy for Investigating Adsorbed Species on a Single-Crystal Surface Using Electrochemically Prepared Au Tips," *Applied Physics Letters* 91 (2007): 101105.

55. B. Yang, E. Kazuma, Y. Yokota, and Y. Kim, "Fabrication of Sharp Gold Tips by Three-Electrode Electrochemical Etching With High Controllability and Reproducibility," *Journal of Physical Chemistry C* 122 (2018): 16950–16955.

56. A. Hartschuh, E. J. Sanchez, X. S. Xie, and L. Novotny, "High-Resolution Near-Field Raman Microscopy of Single-Walled Carbon Nanotubes," *Physical Review Letters* 90 (2003): 095503.

57. T. Yano, T. Ichimura, S. Kuwahara, et al., "Tip-Enhanced Nano-Raman Analytical Imaging of Locally Induced Strain Distribution in Carbon Nanotubes," *Nature Communications* 4 (2013): 2592.

58. A. Taguchi, N. Hayazawa, K. Furusawa, H. Ishitobi, and S. Kawata, "Deep-UV Tip-Enhanced Raman Scattering," *Journal of Raman Specroscopy* 40 (2009): 1324–1330.

59. D. K. Gramotnev and S. I. Bozhevolnyi, "Plasmonics Beyond the Diffraction Limit," *Nature Photonics* 4 (2010): 83–91.

60. F. Lu, W. Zhang, L. Huang, et al., "Mode Evolution and Nanofocusing of Grating-Coupled Surface Plasmon Polaritons on Metallic Tip," *Opto-Electronic Advances* 1 (2018): 180010.

61. R. Yadav, T. Umakoshi, and P. Verma, "Numerical Characterization of Optical Properties of Tapered Plasmonic Structure on a Cantilever Pyramidal Tip for Plasmon Nanofocusing," *AIP Advances* 12 (2022): 085216.

62. R. Yadav, H. Arata, T. Umakoshi, and P. Verma, "Plasmon Nanofocusing for the Suppression of Photodegradation in Fluorescence Imaging Using Near-Field Scanning Optical Microscopy," *Optics Communications* 497 (2021): 127206.